



HAL
open science

Deformation of a chalcogenide glass film under optical modulated excitation

Janine Emile, Yann Gueguen, Jean-Christophe Sangleboeuf, Virginie Nazabal,
O. Emile

► **To cite this version:**

Janine Emile, Yann Gueguen, Jean-Christophe Sangleboeuf, Virginie Nazabal, O. Emile. Deformation of a chalcogenide glass film under optical modulated excitation. *Journal of Non-Crystalline Solids*, 2020, 535, pp.119962. 10.1016/j.jnoncrysol.2020.119962 . hal-02796936

HAL Id: hal-02796936

<https://hal.science/hal-02796936>

Submitted on 11 Jun 2020

HAL is a multi-disciplinary open access archive for the deposit and dissemination of scientific research documents, whether they are published or not. The documents may come from teaching and research institutions in France or abroad, or from public or private research centers.

L'archive ouverte pluridisciplinaire **HAL**, est destinée au dépôt et à la diffusion de documents scientifiques de niveau recherche, publiés ou non, émanant des établissements d'enseignement et de recherche français ou étrangers, des laboratoires publics ou privés.

Deformation of a chalcogenide glass film under optical modulated excitation

Janine EMILE^a, Yann GUEGUEN^a, Jean-Christophe SANGLEBOEUF^a,
Virginie NAZABAL^{b,c}, Olivier EMILE^{d,1,*}

^aUniversité de Rennes 1, CNRS IPR UMR 6251, F-35000 Rennes, France

^bUniversité de Rennes 1, CNRS ISCR UMR 6226, F-35000 Rennes, France

^cDepartment of Graphic Arts and Photophysics, Faculty of Chemical Technology,
University of Pardubice, 53210 Pardubice, Czech Republic

^dUniversité de Rennes 1, F-35000 Rennes, France

Abstract

We report a significant thinning of an amorphous chalcogenide film (at least 5 % of its initial thickness) from the Ge-Sb-Se system deposited by RF magnetron sputtering method on a borosilicate substrate, namely a BK7. This phenomenon is due to a resonant symmetric vibration mode at a low frequency, in the tens of Hertz range. By exciting the material with modulated near-infrared light ($\lambda = 1.55 \mu\text{m}$), we observe three transmission peaks of a probing light at slightly different frequencies of modulation. We assign these resonances to the air/chalcogenide, chalcogenide/BK7 and BK7/air interfaces. Under the effect of the optical modulated radiation pressure, the mechanical deformations of these interfaces show the contribution of associated surface tensions.

Keywords: Chalcogenide glass, surface tension, mechanical resonance, optical excitation, thin film.

Highlights

- Optical modulated radiation pressure inducing interfacial deformations of solid films
- Resonant mechanical vibrations in a thin chalcogenide glass

*Corresponding author

¹mail: emile@univ-rennes1.fr

- Thickness oscillations measured by optical interferometry
-

1. Introduction

Every physical structure has frequencies at which it naturally vibrates, known as resonant frequencies. The most popular example of such a resonance is probably the breaking of a crystal glass with a singer's voice [1]. Conversely, these resonances can generate sounds and thus can be used as musical instruments [2]. Moreover, resonance frequencies enable the learning about internal friction and sources of excess dissipation in mechanical sensors [3]. Besides, resonant vibration is a well-established non-destructive technique for the calculation of elastic moduli and internal friction [4, 5, 6, 7, 8]. However, in most of these cases, resonant frequencies belong to the kilohertz range or above and correspond to antisymmetric stretching mode vibrations. Nevertheless, it has been recently evidenced that a symmetric squeezing mode (or breathing mode) can be excited in soap films [9, 10], with a low frequency in the tens of Hertz range. The excitation is performed with a low power modulated laser in the tens of milli-Watt range. It is based on the deformation induced by the radiation pressure of light. One may then wonder whether such resonant vibrations could be generated in solid films, such as glass films, without generating fractures. This letter presents the first investigations of resonant excitation vibrations on a thin chalcogenide glass under modulated laser excitation in low frequency range. Chalcogenide material was chosen by its remarkable optical properties (broad transmission window, large refractive index, non-linear effects). This material is also known to be malleable when heated above its glass transition facilitating the fabrication of thin film devices [11, 12, 13].

2. Materials and Methods

In order to investigate this issue, we have built the following interferometer (see figure 1). A 293 nm thick chalcogenide thin glass film is deposited on a 1-mm thick borosilicate glass substrate (BK7 from Schott). $\text{Ge}_3\text{Sb}_{36}\text{Se}_{61}$ amorphous film was fabricated by RF magnetron co-sputtering technique employing two targets of GeSe_2 and Sb_2Se_3 [14]. Chemical composition of co-sputtered films was determined by energy-dispersive X-ray spectroscopy

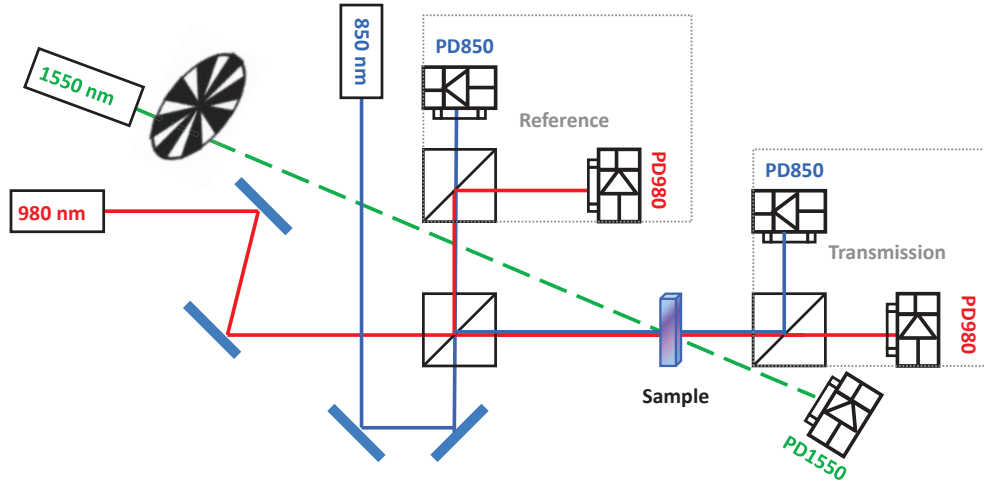


Figure 1: Experimental set-up: the laser light at $\lambda = 1550$ nm is modulated by a chopper and focused on the sample. An interferometric technique measures the sample thickness using the transmitted intensities of two laser diodes at $\lambda = 980$ nm and $\lambda = 850$ nm, normalized to a reference signal. PD: photodiodes for the two studied wavelengths. The photodiodes placed before the sample (reference) measure the laser fluctuations of diodes, in order to correct the experimental transmission from diode laser fluctuations.

joined with scanning electron microscope (JEOL JSM7100F EDS/EBS Oxford), with a precision on the co-sputtered films composition of $\pm 1\%$. The films were as-deposited not annealed. The films were also checked by X-ray diffraction (PANalytical, Almelo, The Netherlands, Cu K-L2,3 radiation, $\lambda = 1.5418$ Å, PIXel1D detector) to control that they are amorphous. The optical refractive indices of selenide glass were determined from variable angle spectroscopic ellipsometry (VASE, J. A. WoollamCo., Inc, Lincoln, NE, USA) at angles of incidence 50° and 60° .

Using different spectroscopic techniques, the film quality has been defined, giving a surface roughness around 0.4 ± 0.2 nm, with a thickness uniformity. Surface topography measurements were carried out using amplitude-modulated atomic force microscope (AM-AFM, Solver Next, NT-MDT Co., Moscow, Russia) with scanned area of $5 \times 5 \mu\text{m}^2$. Unlike liquid films, we were not able to obtain free suspended chalcogenide thin film without damaging it.

By convention, on an interface, the first material that appears on the characterization of the interface corresponds to the material where the light

rays come from. Thus on an air/chalcogenide interface, the light comes from the air and goes to the chalcogenide film. An infrared laser (Keopsys, wavelength $\lambda = 1550$ nm, power $P = 1$ W) bends the air/chalcogenide interface. Indeed, because of the variation index between the two media, a force is induced that goes from the higher index media towards the lower index media. This force writes [15]

$$\vec{F} = N(n_1 - n_2)\hbar\vec{k} = (n_1 - n_2)\frac{P}{h\nu}\hbar\vec{k} \quad (1)$$

where N is the number of photons impinging on the interface per second, $n_2 = 3.18$ and $n_1 = 1$ are the optical index of the chalcogenide film and the air, respectively, and $\hbar = h/2\pi$ is the reduced Planck constant. ν is the optical frequency, P the optical power and \vec{k} is the wavevector ($k = 2\pi/\lambda = 2\pi\nu/c$, c is the velocity of light in vacuum, $\hbar k/h\nu = 1/c$). With our experimental values, this leads to a force of the order of $F = 7.3 \times 10^{-9}$ N. The irradiated surface of the sample is 2.8×10^{-7} m² corresponding to a radius of twice the waist size ($w_0 = 0.3$ mm) for the excitation laser. The resulting pressure also called optical radiation pressure is $p = F/(\pi w_0^2) = 2.6 \times 10^{-2}$ Pa.

The force by itself, and thus the pressure, is too low to induce any significant bending of the air/chalcogenide interface. We have thus used parametric amplification resonance. We modulate the light intensity with a chopper at an adjustable frequency f and we look for a resonance frequency at which the sample response is significant.

The film thickness is measured using an interferometric technics [16]. The instrumental resolution (of the order of a fraction of nanometer) is much more accurate than the film thickness (typically a hundred nanometers). As the thickness of the film varies, the optical pass of the various rays reaching the photodiodes (some of the rays undergoes several reflections) varies, leading to constructive or destructive interferences and thus to fringes on the photodiodes. This leads to a modulation of the transmitted signal as the thickness changes. Then, using the interferences of two laser diodes ($\lambda = 850$ nm and $\lambda = 980$ nm, laser intensity 1 mW/mm²), one can thus deduce the variation of the film thickness (see section 3). The whole experimental set up lies in air on an anti-vibrating table.

The light beam is modulated with a chopper. The input signal sent to the chopper is computer generated with an accuracy of 0.1 mHz, and is checked with a frequency meter. At a given modulation frequency, we register the

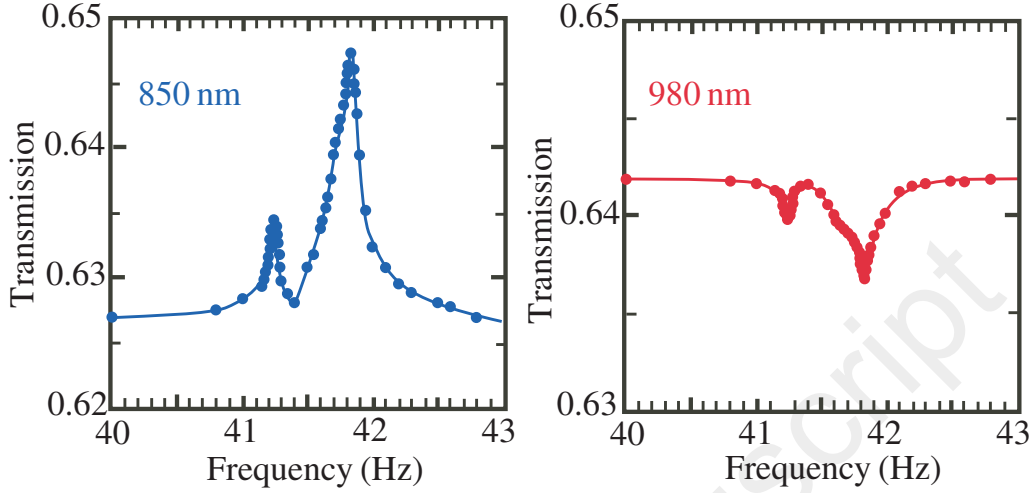


Figure 2: Measured transmissions of the two laser diodes a) $\lambda = 850$ nm, and b) $\lambda = 980$ nm, versus the modulation frequency of the laser responsible for the deformation.

transmission of the two laser diodes during 200 s. We then correct for the fluctuations of the diode lasers with the reference signal. We switch off the modulated laser and wait for 200 s more before switching on the laser again, and thus exciting the sample. We vary the modulation frequency f from 20 to 100 Hz, with a 0.01 Hz step. We repeated experiments to ensure the reproducibility of data and noticed a gradual degradation of the chalcogenide film that falls off the substrate. In this later case, the results are no more reproducible and the film shortly breaks if we continue to excite the system.

3. Results

The transmitted intensity of the two probe beams versus the modulation frequency appears on figure 2. One clearly see two resonances at $f = 41.24 \pm 0.01$ Hz and $f = 41.83 \pm 0.01$ Hz, and a small shoulder at $f = 41.50 \pm 0.05$ Hz. These two main resonances are narrow with a Q-factor around ten. In addition, we observed that the thickness variation process is not instantaneous. Besides, when the modulation is switched off, the sample returns to equilibrium after 15 s. We didn't notice any thickness variation at twice ($2f$) or three times the resonant frequency ($3f$).

From the transmission curves of figure 2, one can deduce the deformation of the thin glass film. Let us consider, from a theoretical point of view, the

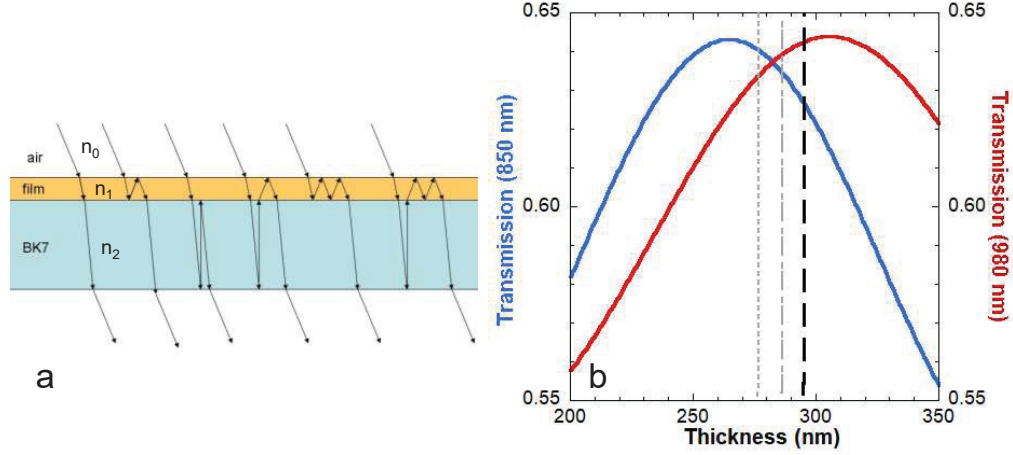


Figure 3: a) Principle of the calculation: the various paths interfere constructively or destructively. b) Theoretical transmissions for the two laser diodes. From the experimental data of figure 2, the thinning of the chalcogenide film is deduced. The bold dashed line corresponds to the initial 293 nm-thickness. The next dashed line is for the thinning, at a modulation frequency of 41.24 Hz, the dotted line is for 41.83 Hz.

transmission of the layer depicted on figure 3. The transmission results from the interference of several rays. For example, one can follow the ray that is transmitted through each interface (numbered 1 in figure), the one that is reflected on the chalcogenide/substrate interface, then on the chalcogenide/air interface and then goes straight (numbered 2), the one that is transmitted through the chalcogenide film, reflected on the substrate/air interface, then on the substrate/chalcogenide interface (numbered 3), and so on.

One can evaluate the theoretical transmission in amplitude. We model the sample as a stack of air, chalcogenide film and a BK7 substrate, with refractive indices n_0 , n_1 and n_2 respectively. $n_0 = 1$, $n_2 = 1.5$ but n_1 depends on the wavelength ($n_1(\lambda_1 = 850 \text{ nm}) = 3.48$ and $n_1(\lambda_2 = 980 \text{ nm}) = 3.35$). The reflection and transmission coefficients between the air and the film are $r_{01} = (n_1 n_0)/(n_1 + n_0)$ and $t_{01} = 2n_0/(n_0 + n_1)$ respectively, they are $r_{12} = (n_1 n_2)/(n_1 + n_2)$ and $r_{21} = -r_{12}$, and $t_{21} = 2n_1/(n_1 + n_2)$ between the chalcogenide film and the substrate, and are $r_{20} = (n_2 n_0)/(n_2 + n_0)$ and $t_{20} = 2n_2/(n_2 + n_0)$ between the substrate and the air [17]. The transmission of the sample needs to be modeled with respect to the thickness and phase shift of the electric field incident to the stack. The phase shifts are:

$\phi_1 = 2\pi n_1 d_1 / \lambda$ and $\phi_2 = 2\pi n_2 d_2 / \lambda$, where d_1 and d_2 ($d_2 = 1$ mm) are the thicknesses of the film and the substrate, respectively. Figure 3a shows the first six different optical paths that contribute mainly to the total intensity transmission intensity t_{tot} . It writes

$$t_{tot} = \left| \sum_i A_i \right|^2 \quad (2)$$

where :

$$A_1 = t_{01} \times t_{12} \times t_{20}, \quad (3)$$

$$A_2 = t_{01} \times r_{12} e^{-2\phi_1} r_{10} \times t_{12} \times t_{20} \quad (4)$$

$$A_3 = t_{01} \times t_{12} \times r_{20} e^{-2\phi_2} r_{21} \times t_{20} \quad (5)$$

$$A_4 = t_{01} \times t_{12} \times r_{20} e^{-2\phi_2} t_{21} \times r_{10} e^{-2\phi_1} t_{12} \times t_{20} \quad (6)$$

$$A_5 = t_{01} \times r_{12} e^{-2\phi_1} r_{10} \times r_{12} e^{-2\phi_1} r_{10} \times t_{12} \times t_{20}, \quad (7)$$

$$A_6 = t_{01} \times t_{12} \times r_{20} e^{-2\phi_2} t_{21} \times r_{10} e^{-2\phi_1} r_{21} e^{-2\phi_1} r_{10} \times t_{12} \times t_{20} \quad (8)$$

t_{tot} is plotted in figure 3b, for each wavelength, versus the thickness of the chalcogenide glass d_1 , assuming a thinning of the chalcogenide glass only, because the BK7 substrate is orders of magnitude stiffer than the film. Since the chalcogenide glass thickness is below 300 nm, one can deduce, from the correlation of the variation of the two wavelengths, i) the initial thickness that equals $d_1 = 293 \pm 0.5$ nm; ii) the mean thickness variation during excitation by modulated light. For $f = 41.24$ Hz, the 293 nm-thick film experiences a thinning of $\Delta d_1 = 7 \pm 0.5$ nm, and for $f = 41.83$ Hz, the 293 nm-thick film experiences a thinning of $\Delta d_1 = 16 \pm 0.5$ nm. Since the light flux (probing lasers at 850 nm and 980 nm, modulated laser at 1550 nm) is the same whatever the modulated frequency, and since times associated with thermal effects belongs to the hundreds of second range [18], it precludes the possibility of a deformation due to a temperature increase associated with the light absorption. It is worth noting that the resonance frequency depends on the glass composition. For the same thin film thickness on the same substrate, we have found a resonant frequency $f = 41.61$ Hz instead of $f = 41.83$ Hz, for a $\text{Ge}_{15}\text{Sb}_{22}\text{Se}_{63}$ [19].

This is a mean thinning of the glass thickness. Besides, at resonance, the glass must vibrate at a frequency corresponding to the excitation frequency. This can be evidence with the help of a lock-in amplifier, connected to the output of the signal of the photodiodes. Such a lock-in amplifier extracts a

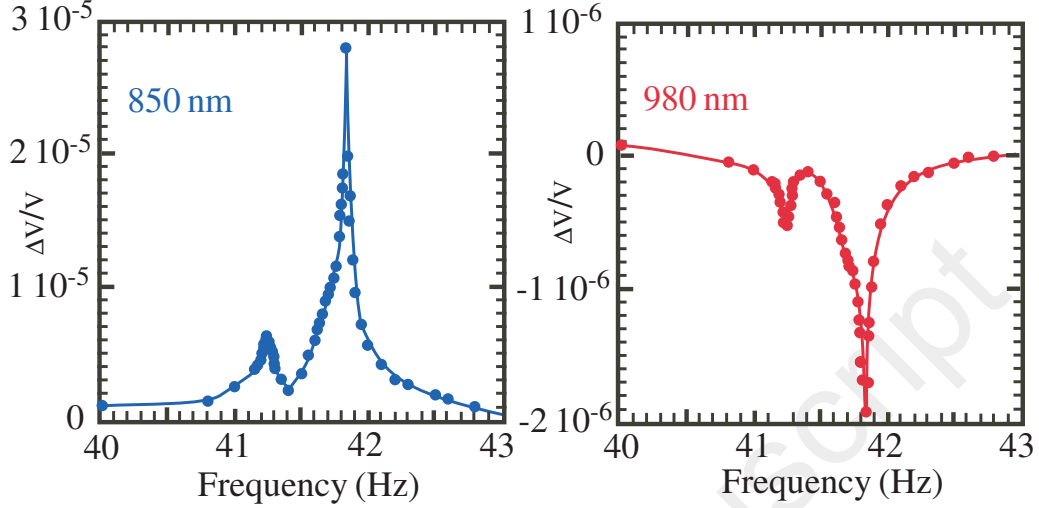


Figure 4: Relative amplitude modulation of the transmitted signal under parametric amplification versus modulation frequency. From figures 2 and 3, one can deduce the amplitude of the modulation of the film thickness. Note that there is a π phase difference between the two amplitudes. This is the reason why the signal on the photodiode for $\lambda = 850$ nm increases whereas the signal on the photodiode for $\lambda = 980$ nm decreases. $\Delta V/V$ is the relative variation of the signal on the photodiode. It is equal to the relative amplitude variation.

tension V of the signal of the photodiode that is proportional to the amplitude of the oscillation. An example of the variation of the relative tension $\Delta V/V$ on the photodiode and thus of the light transmission versus the excitation frequency is displayed in figure 4.

One can then deduce the amplitude of the oscillation of the film thickness. For example at resonance, for $f = 41.83$ Hz, the relative amplitude modulation is 3×10^{-5} . From figure 3, a variation of the mean signal of 4% corresponds to a thinning of $\Delta d_1 = 16$ nm. The amplitude of the vibration is thus 12 ± 0.5 pm at resonance. Note that there is three orders of magnitude difference between the mean thinning of the film and the amplitude of the vibration of the film.

We have here evidenced the resonance behavior with two different experiments. On the one hand, we have demonstrated resonances in thinning of the chalcogenide film. On the other hand we have shown resonances in the vibration amplitude of the same chalcogenide film. The resonant frequencies are exactly the same and the resonance curves are alike, with the same Q-

factor. This confirms the existence of such a resonance. It is worth noting that the vibration of the film is induced via the chopped light. There is no mechanical excitation nor mechanical modulator. The detection is performed thanks to a photodiode via a lock-in amplifier. Out of resonance we didn't register any vibration of the system.

4. Discussion

The resonant frequency is very low (in the tens of Hz) compared with usual resonant frequencies of glass samples that lay in the kilo-Hertz range or higher [3, 6, 7, 20]. These high frequency resonances, corresponds to an antisymmetric vibration mode. They are specific of the elastic properties of glass materials and are used to calculate Young's modulus and Poisson's ratio. For free-standing liquid films, the antisymmetric mode (where the air/liquid interfaces vibrate in phase) is commonly observed and the film keeps a constant thickness. The symmetric mode (breathing mode where the air/liquid interfaces vibrate out of phase), with thickness modulations, has been only observed in a low frequency range using the parametric amplification [9, 10].

We have performed finite element analysis (FEA) on the glass thin film, without simulating the substrate because of the large number of elements required for such simulation. The film has been simulated in axisymmetric mode, with the pressure imposed as a gaussian distribution corresponding to the laser intensity distribution, on the top of the film. The bottom of the film was fixed with no degree of freedom (but simulations were also done with all the degree of freedom, and with pressure on both sides). The thickness used was the one of the film (293 nm), and the diameter 5 times the laser beam radius (1.25 mm). The pressure was imposed as a rectangular wave, during 20 periods with 100 steps per period, and simulation were done with frequencies between 1 and 100 Hz every 0.1 Hz. The chalcogenide glass was first simulated as an isotropic linear elastic material (Young's modulus: 21.6 GPa, Poisson's ratio: 0.269, density: 4.95 g/cm³[21]) and then as an isotropic linear viscoelastic material with a least a relaxation time near 0.025 s (close to the inverse of the expected resonance frequency). None of these simulations show any resonance at any frequency, suggesting that the mechanism involved is neither due to the elasticity nor the viscosity of the glass thin film, but a mechanism not taken into account in our simulation, namely: the surface tension. Whatever the symmetry of the excited modes, the vibrations are

mediated by the surface tension. Is there any such parameter that can be identified in the case of glasses?

4.1. Influence of the surface tension.

Actually the surface tension of chalcogenide glasses is a key parameter of crystallization process in glass forming. Nevertheless experimental determinations are scarce. Numerical estimations have shown that it should be around $\gamma = 0.2$ N/m for Ge-Sb-Se glass compositions [22]. The surface tension acts as a spring force on the air/chalcogenide interface. Then the sample (chalcogenide thin film and substrate) can be modeled as a harmonic oscillator and the resonance frequency can be written as

$$f = \frac{1}{2\pi} \sqrt{\frac{\gamma}{m}} \quad (9)$$

where m is the effective mass. Indeed, this mass is calculated from the density ($\rho = 2.52$ g.cm⁻³) of the chalcogenide film and BK7 support (the sample has been weighted). Since the exciting beam has a Gaussian profile, the irradiated surface corresponds to a surface with a radius that is twice the waist ($S_{ef} = \pi \times (2 \times w_0)^2 = 1.13$ mm²), leading a mass $m = \rho \times e \times S_{ef} = 2.85 \times 10^{-6}$ kg, i.e. approximately $m = 3 \times 10^{-6}$ kg ($e = 1$ mm is the BK7 thickness). This leads to a resonance frequency $f = 41.1 \pm 1$ Hz. This is the correct order of magnitude of the resonance frequency compared with what we found experimentally. It is thus likely that, as for the free standing liquid films, the surface tension is the leading parameter of the mechanical response of the film under parametric amplification oscillation. Then, the experimental determination of the resonant frequency under modulated excitation could be a very new method to investigate the surface tension of various glass materials. Nevertheless, we face an other problem that is the existence of two very close resonant peaks in the response of the film.

One possible explanation is that this double resonance peak could be due to a non-homogeneous composition in the chalcogenide thin film related to the co-sputtering deposition technique. Indeed, thin films from two different targets of GeSe₂ and Sb₂Se₃ may not be perfectly homogeneous related to slightly different deposition rates, dissimilar sputtered energies and recombination of atoms and clusters on the surface of the substrate. But these effects are at a scale not observable by scanning electron microscope analysis suggesting that the layer is homogeneous in its composition. This double

peak could be the result of a mechanically induced amorphous-crystalline transformation as for the change in conductivity even if its composition is relatively stable against crystallization [23, 24]. Both phases would vibrate with their own frequency.

It could also be that, since these stoichiometric thin films are made of several bonds [14] mainly Ge–Se, Sb–Se, respecting the stoichiometry of the main $[\text{GeSe}_{4/2}]$ and $[\text{SbSe}_{3/2}]$ entities forming the glass network and in small proportion incorporating Ge–Ge, Sb–Sb, Sb–Ge, Se–Se bonds, the mechanical vibration optically induced is a probe of the presence of different structural entities having relatively varied binding energies linked in a diverse way, creating many free volumes in the amorphous network.

4.2. Existence of several peaks.

However, we think that the emergence of several resonances peaks is due to the existence of several interfaces with different surface tensions, experiencing different solicitations. In particular the forces are different. For a given incident power P , on a interface between two media of different indexes n and n' , the reflected power P_R writes [17]

$$P_R = \left(\frac{n - n'}{n + n'} \right)^2 P \quad (10)$$

The transmitted power P_T is then $P_T = P - P_R$. One could have calculated the reflected and transmitted powers using previous equations (equation 2 to 8). However, these previous calculations are dedicated to determining the interferences which mainly occur in thickness variations. The powers are modulated with the film thickness, with a 5% amplitude. Here we evaluate the order of the magnitude of the mean force, there is no need to consider all the paths, only the first reflection in figure 3a is considered.

Then on the air/chalcogenide interface, the incident power is 1 W. The transmitted power is 0.73 W, the reflected power is 0.27 W. The reflected light acts on the interface. The force is $F_R = 2 \times 0.27 \times P/c = 1.8 \times 10^{-9}$ N. This force is the usual radiation pressure force acting on a mirror. It is in the same direction of the incident light and opposed to the direction of the reflected light. It is thus directed from air towards the chalcogenide film. The factor of two accounts for that each incident photon transfer $\hbar k$ to the interface and $\hbar k$ while reflected. According to equation 1, the change of index at the interface leads to a force $F = (n_2 - n_1) \times 0.73 \times P/c = 5.3 \times 10^{-9}$ N. It is directed from the higher index medium towards the lower index medium. On

Table 1: Experimental values of the force F , the resonant frequency f and surface tension of air/chalcogenide interface (Chal/air), chalcogenide/BK7 substrate interface (Chal/BK7), and BK7/air interface (BK7/air).

	Force ($\times 10^{-9}$ N)	f (Hz)	γ (N/m)
Chal/air	3.5	41.24	0.201
Chal/BK7	4.3	41.83	0.207
BK7/air	1.1	41.7	0.206

the air/chalcogenide interface, it is directed from the chalcogenide towards the air. The resultant force is then 3.5×10^{-9} N.

On the chalcogenide/substrate interface, the reflected power is $0.18 \times 0.73 = 0.13$ W. The force is then 0.9×10^{-9} N. As previously, it is in the direction of the incident light, i.e. from the chalcogenide towards the substrate. The transmitted power is $0.82 \times 0.73 = 0.6$ W, leading to a force of 3.4×10^{-9} N, directed from the higher index medium towards the lowest index medium, i.e. from the chalcogenide towards the BK7. The two forces act in the same direction. The resultant force is 4.3×10^{-9} N, directed from the chalcogenide towards the BK7. Analogously, the resultant force on the BK7/air interface equals 1.1×10^{-9} N (see table 1), and is directed from the BK7 towards the air.

The surface tensions on each interface are of course different, and the forces are also different. According to the values of the forces, we assign the first resonant peak at $f = 41.24$ Hz to the air/chalcogenide interface, the second peak at $f = 41.83$ Hz to the chalcogenide/BK7 interface. Looking closer to this last peak, it is composed of two peaks, one leading peak at $f = 41.83$ Hz, and another smaller peak at $f = 41.8$ Hz. We assign this last peak to the BK7/air interface.

Then, according to Eq. 9, we are able to determined the different surface tensions. The surface tension γ of the air/chalcogenide interface equals $\gamma = 0.201$ N/m, the surface tension of the chalcogenide/BK7 interface equals $\gamma = 0.207$ N/m, and the surface tension of the BK7/air equals $\gamma = 0.206$ N/m (see table 1). Then knowing precisely the mass of the substrate, we are able to evaluate the surface tensions with a very high accuracy. Nevertheless, if there is a lower accuracy on the mass, and if one of the surface tension is known, the other ones can be deduced readily since their ratio depends only of the frequency ratio and doesn't depend on the mass.

It is worth noting that the determination of the surface tension is a highly debated issue [25, 26]. Experimental values are usually obtained close to the glass/liquid temperature transition and then assumed to be independent of the temperature. Theoretical values results from model calculating the energy needed to break bounds at the interface [27], leading to macroscopic fractures, whereas, in our case, the nanometric deformations are indeed reversible, with a recovering time, as already mentioned that is about 15 s. Our experimental results, together with the low frequency vibration resonance technics may shine some new light on the surface tension of solids, and on the deformation of solids more generally.

4.3. Photoinduced effects

Chalcogenide glasses are known to undergo photoinduced effects under light irradiation with photon energies close to their optical band-gap, such as photocontraction [28].

The band-gap of the chalcogenide glass used here, calculated using the Tauc's model [29] is 1.43 eV [19], far above the 0.8 eV of the laser light at 1550 nm. Nevertheless in amorphous materials, the presence of energy band tails results in significant absorption event at photon energies below the optical band-gap. The photon energies used here may not be sufficient to induce significant photoinduced effects [14].

Additionally, it has never been observed that pulse irradiation at such a low frequency could induce a resonance effect through photoinduced structural changes: pulse irradiation at tens of Hz will induce the same effect as a continuous irradiation [30], and if it existed, an identical photocontraction at all frequencies, with no resonance. Finally, photoinduced effect are at least partially irreversible, whereas the effect observed here is fully reversible. Consequently, we can assume that the deformation observed here is not related to any photoinduced effect as usually described in chalcogenide glasses.

4.4. Viscoelasticity

As indicated previously, the nanometric deformations observed are reversible, with a recovering time of about 15 s. Such a time dependent deformation is typical of a viscoelastic deformation. The experiment was done far below the glass transition temperature ($\sim 512K$), so we could assume that the film is purely elastic. But thin films are known to be far away from equilibrium and could thus exhibit a viscoelastic behavior even at room

temperature [31]. Further investigations are necessary to determine the viscoelastic properties of the thin film, and to support this hypothesis.

5. Conclusions

We have evidence a symmetrical vibration mode of a thin chalcogenide film with chemical composition of $\text{Ge}_{15}\text{Sb}_{22}\text{Se}_{63}$ deposited on a BK 7 substrate. The phenomenon results from a modulated mechanical excitation action originating from the radiation pressure of light. The fact that the film is not freely suspended has led to the observation of three resonance peaks at low frequencies between 41 and 42 Hz. By calculating, in an optical ray model, the different optical paths through the chalcogenide and substrate layers, we have estimated a thinning of 16 nm and 7 nm associated respectively with the air/chalcogenide and chalcogenide/BK7 substrate interfaces. Using a lock-in amplifier, we measured thickness amplitudes vibrations of the order of ten picometer.

For a given a resonance frequency range, we explained these mechanical deformations by the contribution of the surface tension, a parameter previously mostly ignored in finite element model calculations. This work needs to be pursued by studying other chalcogenide glasses of different compositions and deposited on other types of substrates to probe the adhesion properties with very high accuracy. Such investigations are currently carried out.

Acknowledgments: The authors thank Vincent BURGAUD, Elfrich GONZALES AREVALO and Mickaël LE FUR (IPR, Université de Rennes 1) for technical support, and the Centre National de la Recherche Scientifique (CNRS) for financial support within the framework of a défi émergent.

Bibliography

- [1] B. Berner. Resonant wineglasses and Ping-Pong balls. *Phys. Teach.* **38**, (2000) 269.
- [2] D.A. Gallo, S. Finger. The power of a musical instrument: Franklin, the Mozarts, Mesmer, and the glass armonica. *History Psychol.* **3**, (2000) 326.
- [3] W. J. Startin, M. A. Beilby, and P. R. Saulson. Mechanical quality factors of fused silica resonators. *Rev. Sci. Inst.* **69**, (1998) 3681.

- [4] G. Martincek. The determination of Poisson's ratio and the dynamic modulus of elasticity from the frequencies of natural vibration in thick circular plates. *J. Sound Vibration* **2**, (1965) 116.
- [5] M. Lalanne, O. Berthier, J. der Hagopian J. *Mechanical Vibration for Engineers*. (John Wiley, New York, 1983).
- [6] P. Gadaud and S. Pautrot. Characterization of the elasticity and anelasticity of bulk glasses by dynamical subresonant and resonant techniques. *J. Non-Cryst. Solids* **316**, (2003) 146.
- [7] T. Rouxel. Elastic properties and short-to medium-range order in glasses. *J. Am. Ceram. Soc.* **90**, (2007) 3019.
- [8] A. Vega-Flick, N. W. Pech-May, F. Cervantes-Alvarez, and J. J. Alvarado-Gil. Vibrations of micron-sized fluid membranes induced via pulsed laser excitation. *J. Fluid. Struct.* **81**, (2018) 58.
- [9] O. Emile and J. Emile. Laser-induced vibration of a thin soap film. *Lab on a Chip* **14**, (2014) 3525.
- [10] O. Emile and J. Emile. Towards an optofluidic pump? *Optofluid. Microfluid. Nanofluid.* **3**, (2016) 49.
- [11] A. Zakery and S. R. Elliott. *Optical nonlinearities in chalcogenide glasses and their applications*. (New York: Springer 2007).
- [12] K. Tanaka and K. Shimakawa. *Amorphous chalcogenide semiconductors and related materials*. (Springer Science and Business Media, 2011).
- [13] J.L. Adam and X. Zhang. *Chalcogenide glasses: preparation, properties and applications*. (Woodhead publishing, 2014).
- [14] T. Halenkovič, J. Gutwirth, P. Němec, E. Baudet, M. Specht, Y. Gueguen, J.C. Sangleboeuf, and V. Nazabal. Amorphous Ge-Sb-Se thin films fabricated by co-sputtering: Properties and photosensitivity. *J. Am. Ceram. Soc.* **101**, (2018) 2877.
- [15] O. Emile and J. Emile. Energy, linear momentum, and angular momentum of light: what do we measure?. *Ann. Phys.* **530**, (2018) 1800111.

- [16] J. Emile, F. Casanova, G. Loas, and O. Emile. Swelling of foam lamella in a confined channel. *Soft Matter* **8**, (2012) 3223.
- [17] M. Born and E. Wolf. *Principle of Optics* 7th Ed. (Cambridge University Press, London, 1999).
- [18] M. Buisson, Y. Gueguen, R. Laniel, C. Cantoni, P. Houizot, B. Bureau, J. C. Sangleboeuf, and P. Lucas. Mechanical model of giant photoexpansion in a chalcogenide glass and the role of photofluidity. *Physica B: Condens. Matter* **516**, (2017) 85.
- [19] M. Specht. *Comportement mécanique de films minces de calcogénures sous irradiation de photons* (Doctoral dissertation, Rennes 1, 2017).
- [20] S. Bossuyt, S. Giménez, and J. Schroers. Resonant vibration analysis for temperature dependence of elastic properties of bulk metallic glass. *J. Mater. Res.* **22**, (2007) 533.
- [21] A.N. Sreeram, A.K. Varshneya, and D.R. Swiler. Molar volume and elastic properties of multicomponent chalcogenide glasses. *J. Non-Cryst. Solids* **128**, (1991) 294.
- [22] T. D. Melnichenko, V. I. Fedelesh, T. N. Melnichenko, D. S. Sanditov, S. S. Badmaev, and D. G. Damdinov. On the approximate estimation of the surface tension of chalcogenide glass melts. *Glass Phys. Chem.* **35**, (2009) 32.
- [23] G. C. Vezzoli, P. J. Walsh, and L. W. Doremus. Threshold switching and the on-state in non-crystalline chalcogenide semiconductors: An interpretation of threshold-switching research. *J. Non-Cryst. Solids* **18**, (1975) 333.
- [24] A. L. Greer and N. Mathur. Materials science: Changing face of the chameleon. *Nature* **437**, (2005) 1246.
- [25] R. W. Style, A. Jagota, C. Y. Hui, and E. R. Dufresne. Elastocapillarity: Surface tension and the mechanics of soft solids. *Annu. Rev. Condens. Matter Phys.* **8**, (2017) 99.
- [26] J. Bico, E. Reyssat, and B. Roman. Elastocapillarity: When surface tension deforms elastic solids. *Annu. Rev. Fluid Mech.* **50**, (2018) 629.

- [27] T. Rouxel and S. Yoshida. The fracture toughness of inorganic glasses. *J. Am. Ceram. Soc.* **100**, (2017) 4374.
- [28] Kolobov, A. V. (Ed.). (2006). Photo-induced metastability in amorphous semiconductors. John Wiley & Sons.
- [29] D. L. Wood and J. S. Tauc. Weak absorption tails in amorphous semiconductors. *Phys. Rev. B* **5**, (1972) 3144.
- [30] P. Lucas, E.A. King and A. Doraiswamy (2006). Comparison of photostructural changes induced by continuous and pulsed laser in chalcogenide glass. *J. Optoelectron. Adv. Mater.* **294**, (2006) 776.
- [31] Y. Gueguen, J.-C.Sangleboeuf, V. Keryvin, T. Rouxel, E.A. King, E. Robin, G. Delaizir, B. Bureau, X.-H. Zhang and P. Lucas, Sub-Tg viscoelastic behaviour of chalcogenide glasses, anomalous viscous flow and stress relaxation. *J. Ceram. Soc. Jpn.* **116**, (2008) 890